

## COLLECTIVE ROTATIONS IN OXIDES

EMILIO ARTACHO

*Departamento de Física de la Materia Condensada, C-III  
Universidad Autónoma de Madrid, 28049 Madrid, Spain*

KANWAL G. SINGH

*Department of Physics, Wellesley College, Wellesley, MA 02181, USA*

GUILLERMO GOMEZ-SANTOS

*Departamento de Física de la Materia Condensada, C-III  
Universidad Autónoma de Madrid, 28049 Madrid, Spain*

Based on bond arguments, a Hamiltonian is introduced to describe the fundamental physics of the collective rotations of oxygen atoms in oxides. Values for the relevant material parameters are estimated for silica and Cu oxides. Zero-temperature phase diagrams are presented; the different phases and associated transitions are characterized. Phases with non-phononic excitations are found.

### 1 Introduction

The tendency of oxygen atoms to form just two bonds with a bond angle smaller than  $180^\circ$  allows the appearance of low energy atomic motions related to internal rotational degrees of freedom which, in a first approximation, involve neither bending nor stretching of bonds (“rigid unit modes” in silicates, “floppy modes” in glasses).<sup>1</sup> A huge variety of compounds exhibit the oxygen-bridge  $X-O-X$  basic unit,  $X$  being a linking atom. Among the many silicates,  $\beta$ -cristobalite (a silica polymorph) shows these internal rotations most clearly.<sup>1</sup> The perovskites are also interesting candidate materials, especially the  $\text{CuO}_2$  planes of the high  $T_c$  superconducting materials.

### 2 Model and Hamiltonian

A lattice of fixed  $X$  atoms is considered with O atoms bridging between them. The degrees of freedom are the angles  $\phi_i$  associated with the oxygens in their rotations around the axes defined by the neighboring nodes (given a fixed  $X$ -O distance those rotations are the only possible motions). The Hamiltonian is

$$\mathcal{H} = -B \sum_i \partial^2 / \partial \phi_i^2 + 2t \sum_{\langle i,j \rangle} \cos(\phi_i - \phi_j) - 2C \sum_i \cos(n\phi_i), \quad (1)$$

including the kinetic energy, a nearest neighbor interaction which tends to align the O bridges ( $t > 0$ ), and a hindering potential. The latter accounts for effects in real solids which impede the rotation of the oxygen atoms. It is a

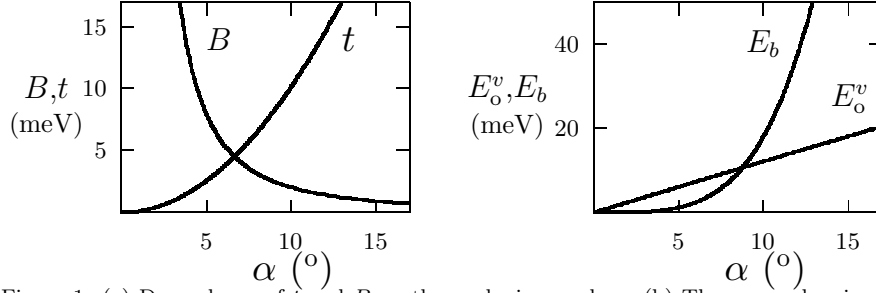


Figure 1: (a) Dependence of  $t$  and  $B$  on the puckering angle  $\alpha$ , (b) The energy barrier  $E_b$  and lowest vibrational energy  $E_o^v$  vs.  $\alpha$  for the radial motion of oxygen. SiO<sub>2</sub> case.

fixed potential, whereas in the real solids the impeding objects (other atoms) are mobile.  $n$  gives the number of potential minima around the circle.

The rotor constant is  $B = \hbar^2/2I$ , where  $I = m_O R^2$ , and  $R = b \sin \alpha$ ,  $b$  being the bond length (1.6 Å for Si-O, 1.9 for Cu-O), and the puckering angle  $\alpha = (\pi - 2\theta_{X-O-X})/2$ . Therefore,  $B = B_o/\sin^2 \alpha$ , with  $B_o \approx 0.06$  meV for Si and 0.04 for Cu. The interaction parameter  $t$  accounts for the energy needed to rotate an O atom while keeping its neighbors fixed. This energy is essentially used to bend the O-X-O angle away from its natural value. Then,  $t = t_o(1 - \cos 2\alpha)$ . Using the O-X-O bond bending force constants,  $t_o \approx 170$  meV for Si, and 230 for Cu.  $B$  decreases with  $\alpha$  whereas  $t$  increases, defining an  $\alpha$  for which  $B = t$  ( $7^\circ$  for Si,  $5^\circ$  for Cu).  $C$  is much more dependent on particular crystal structures and more difficult to estimate. It increases with  $\alpha$ , and can be as small as 0.1 meV for  $\alpha = 20^\circ$ , as found for interstitial O in Ge.<sup>2</sup>

The radial vibration of the O atoms involves the stretching of X-O bonds and can be neglected for well-defined rotor situations. However, for small enough  $\alpha$ , the radial motion becomes important since  $\Delta R \sim \langle R \rangle$ . An estimate of the range of validity of  $\mathcal{H}$  can be drawn from the X-O bond stretching force constants, by comparing the ground-state energy for the radial vibrations  $E_o^v$  with  $E_b$ , the potential energy barrier at  $R = 0$ .  $E_b = K(1 - \cos \alpha)^2$ , with  $K \approx 80$  eV for Si and 30 for Cu.  $E_o^v = K' \sin \alpha$ , with  $K' \approx 70$  meV for Si, 35 for Cu.  $E_b > E_o^v$  for  $\alpha > 9^\circ$  both for Si and Cu. Only the  $\phi_i$  will be considered here, the effects of the radial motion being the subject of future work.<sup>3</sup>

### 3 Phase diagram

For  $C = 0$  we have a one parameter ( $\tilde{t} \equiv t/B$ ) problem. The zero-temperature  $d$ -dimensional quantum Hamiltonian lies in the universality class of the classical

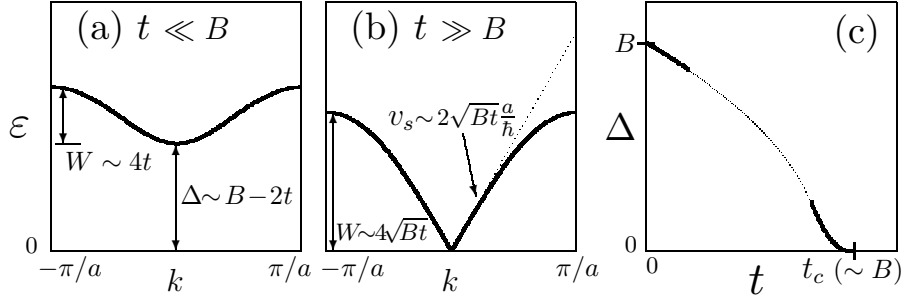


Figure 2: Dispersion relation for the elementary excitations for the 1D Hamiltonian, (a) for  $t \ll B$ , and (b) for  $t \gg B$ . (c) shows the dependence of the gap  $\Delta$  on  $t$ .  $W$ ,  $a$ , and  $v_s$  stand for band width, lattice parameter, and sound velocity, respectively.

$(d+1)$ -dimensional  $XY$  model.<sup>4</sup> This model exhibits a phase transition at some critical  $\tilde{t}_c$  of the order of 1. It is an order-disorder transition for  $d > 1$ , implying a symmetry breaking in  $\phi$  for the ordered phase ( $\tilde{t} > \tilde{t}_c$ ), with its associated long-range order and gapless Goldstone excitations. For  $d = 1$  the transition is of the Kosterlitz-Thouless kind. The  $\tilde{t} > \tilde{t}_c$  “quasi-ordered” phase displays algebraic order ( $\langle e^{i(\phi_i - \phi_j)} \rangle \sim 1/|i - j|^\eta$ , with  $\eta \leq 1/4$ ). The disordered phase shows an exponential decay of  $\langle e^{i(\phi_i - \phi_j)} \rangle$ , with gapped excitations. For  $d = 1$ , near the transition, the gap closes like  $\Delta \sim 1/\xi \sim e^{-K/\sqrt{\tilde{t}_c - \tilde{t}}}$ ,  $\xi$  being the correlation length [Fig.2(c)].

The limits help to understand the nature of the phases. For  $\tilde{t} \ll 1$ , the basis of independent-rotor eigenstates provides a natural language. The interaction term acts like a raising-lowering operator on the rotor quantum numbers  $m_i$ . The original  $\mathcal{H}$  can be mapped<sup>8</sup> into a Hamiltonian of bosonic particles and antiparticles ( $m$  positive or negative) with a chemical potential  $\mu = B$ , a Hubbard-like repulsion  $U = B$ , and a hopping energy  $t$ . Using a Bogoliubov transformation, the  $\tilde{t} \ll 1$  limit can be solved yielding an independent-rotor-like ground state with quantum fluctuations of particle-antiparticle pairs, and rotational excitations (rotatons, dressed rotor excitations), with  $\varepsilon_k = B\sqrt{1 - 4\tilde{t} \cos ka}$  [Fig.2(a)]. For  $\tilde{t} \gg 1$ , a harmonic approximation of the interaction term yields gapless spin-wave-like excitations [Fig.2(b)].

Information for the full phase diagram ( $C \neq 0$ ) can again be obtained from the corresponding classical  $d+1$  model.<sup>4</sup> For  $d = 1$  the phase diagram is displayed in Fig. 3 (a)-(c). In addition to the phases discussed above, a third phase appears, an ordered phase corresponding to the locking of  $\phi$  around one

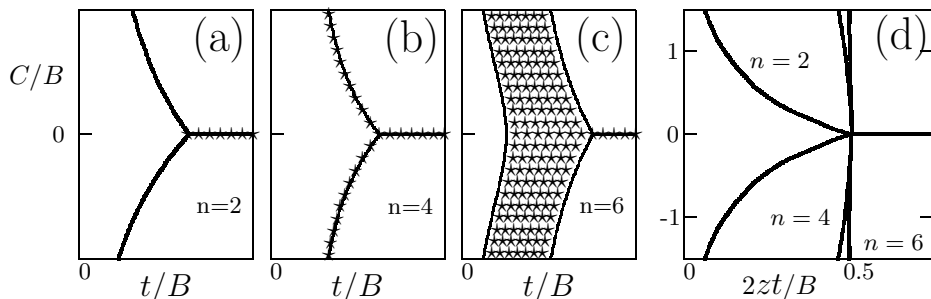


Figure 3: Phase diagrams in the  $C$ - $t$  plane for different values of  $n$ , the number of minima of the hindering potential. (a), (b), and (c) are for one dimension. (d) is obtained from a mean-field approximation, dependent on the coordination  $z$ ; the phase boundaries for  $n=2,4,6$  are indicated in the graph. In every diagram the phase at the left is a disordered phase; the ones at the right, up and down, are ordered phases; stars denote critical points.

of the  $n$  equivalent minima. For  $n > 4$  the critical region separating the ordered and disordered regions has a finite width; it shrinks to a line for  $n = 4$ . For  $n = 2$  the model belongs to the Ising universality class ( $C \neq 0$ ). Indeed, the Hamiltonian maps into a Ising model in a transverse magnetic field for  $C \gg B$ .

A mean-field calculation has been performed to obtain quantitative estimates. We approximate the interaction term by  $4zt \langle \cos \phi \rangle \sum_i \cos \phi_i$ ,  $z$  being the coordination number and  $\langle \cos \phi \rangle$  the order parameter.<sup>5</sup> The phase diagram [Fig. 3(d)] is expected to be more accurate in higher dimensions. The critical regions disappear, with classical order-disorder phase transitions remaining. Higher  $n$  increases the  $C$  range of the disordered phase.

### Acknowledgments

We acknowledge discussions with F. Ynduráin and financial support of DGI-CYT (Spain) grant PB92-0169. KGS was supported by Wellesley College.

### References

- [1] I.P. Swainson and M.T. Dove, *Phys. Rev. Lett.* **71**, 193 (1993).
- [2] E. Artacho and F. Ynduráin, *Mater. Sci. Forum* **196-201**, 103, (1995).
- [3] E. Artacho, K.G. Singh, and G. Gómez-Santos, to be published.
- [4] J.V. José *et al*, *Phys. Rev. B* **16**, 1217 (1977).
- [5] E. Simánek, *Solid State Commun.* **31**, 419 (1979).